Dalton Transactions

COMMUNICATION

View Article Online
View Journal | View Issue

Cite this: *Dalton Trans.*, 2019, **48**, 16869

Received 11th October 2019,
Accepted 4th November 2019

DOI: 10.1039/c9dt04230j

rsc.li/dalton

Synthesis of homoleptic, divalent lanthanide (Sm, Eu) complexes *via* oxidative transmetallation†

Thaige P. Gompa, [a] Ningxin Jiang, [a] John Bacsa [a] and Henry S. La Pierre *[a,b]

The direct synthesis of neutral, divalent samarium and europium complexes supported by the bulky bis(tris-*tert*-butoxysilyl)amide (BTTSA) ligand *via* oxidative transmetallation is reported. Through the use of a copper(I) ligand complex, conventional lanthanide halide starting materials for complex formation are circumvented and the clean formation of divalent complexes is achieved directly from the bulk metal. The structures of the [Ln(BTTSA)$_2$] (Ln = Sm, Eu) complexes are isotypic, presenting divalent lanthanide ions with distorted, six-coordinate geometries.

Synthetic methods for the preparation of lanthanide complexes supported by low-coordination number ligand spheres or high-symmetry planar ligands are crucial technologies for the development and application of molecular lanthanide complexes in quantum information sciences.[1–11] Current approaches rely on salt metathesis reactions which can be complicated by solubility limitations and aggregation issues including the formation anionic, *-ate*, complexes supported by outer sphere alkali counter cations. Oxidative transmetallation can potentially avoid these issues. Historically, this method, in particular the reaction of Cu^{1+} reagents with bulk lanthanide metals, is a synthetic technique that has been explored to prepare lanthanide complexes with small supporting ligands such as cyclopentadienyls (Cp^{1-}), alkynolates ($R–C{\equiv}C^{1-}$), or amides ($[(TMS)_2N]^{1-}$).[12–17] This methodology is related to Hg amalgation and $HgCl_2$ activation procedures for activated metal reactions and to the use alkyl mercurials and thallium in oxidative transmetallation.[14,18–23] It should be noted that these approaches have been combined with an internal base (*e.g.* $Hg(C_6F_5)_2$) to afford the alkali-metal free metallation of bulky, heterotopic calix[4]pyrrole and calix[4]arene ligands in redox transmetallation/protonolysis reactions.[24] Similar methodology and reagents were used to synthesize a number of lanthanide complexes, both di- and trivalent.[25] Further refinement of these techniques has led to applications in the synthesis of organometallic, pentavalent uranium complexes *via* oxidative transmetallation processes using Cu^{1+} or Au^{1+} reagents.[26–28]

Our group is broadly interested in the control of f-block metal oxidation state and valence electronic configuration *via* ligand design.[29,30] In order to design a redox stable ligand, capable supporting lanthanides in a range of oxidation states, a ligand framework incorporating the oxidative stability of tris(*tert*-butoxy)siloxides and the reductive stability and low-coordination number of bulky amides was designed to facilitate the stabilization of monomeric complexes across a range of redox states. This goal was achieved in the synthesis of bis(tris-*tert*-butoxysilyl)amine, **BTTSA**, a bulky monoanionic, polydentate amide ligand. These features help prevent dimerization and, as shown herein, stabilize low-valent lanthanide complexes. The metallation of these bulky ligands is facilitated by oxidative transmetallation.

Synthesis of the bis(tri-*tert*-butoxysilyl)amine, **BTTSA-H**, is shown in Scheme 1. Single crystal XRD confirms the connectivity (Fig. S13†). In contrast to bulky bis(tris-alkyl)silylamides, the Si–N–Si angle is significantly more open at 134.90(7)°, in

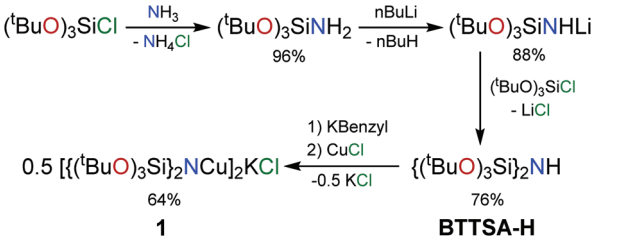

Scheme 1 Multi-step reaction scheme for the synthesis of the copper salt, **1**.

[a]*Department of Chemistry and Biochemistry, Georgia Institute of Technology, Atlanta, Georgia 30332-0400, USA. E-mail: hsl@gatech.edu*
[b]*Nuclear and Radiological Engineering Program, Georgia Institute of Technology, Atlanta, Georgia 30332-0400, USA*

† Electronic supplementary information (ESI) available: Experimental procedures and crystallographic data (PDF and CIF). CCDC 1951786, 1951791, 1951792 and 1953040. For ESI and crystallographic data in CIF or other electronic format see DOI: 10.1039/c9dt04230j

comparison to 126.3(1)° for the lithium salt of bis(*tert*-butyldimethylsilyl)amine.[31] While the size of the silyl substituents changes significantly between the two amines, a key distinction is the incorporation of alkoxide rather than alkyl silyl substituents. The pro-ligand is converted to the active copper(I) species in two steps including deprotonation with potassium benzyl and transmetallation with copper(I) chloride. This copper salt, **1**, is stirred in THF with a glass stir bar over freshly ground lanthanide (Eu or Sm) metal shavings in a 2 : 1 stoichiometric ratio for 60 h to yield the divalent lanthanide complexes **2-Eu** and **2-Sm** in 83% and 68% yield, respectively (Scheme 2).

The molecular structure of **2-Eu** (isotypic to **2-Sm**, whose structure is depicted in Fig. S13†) is shown in Fig. 1 and crystalizes in the $P2_1/n$ space group (Table 1 includes relevant bonding metrics for both complexes). Two *tert*-butoxy arms from each ligand coordinate the metal ion, leading to an overall 6-coordinate ion. Further inspection of the bond metrics reveals uniquely long M–N distances, which on average are 2.712(5) Å and 2.7181(17) Å for **2-Sm** and **2-Eu**, respectively. These are particularly long when compared to the M–N bond lengths in related divalent Sm and Eu amides, which range from 2.483(5) to 2.500(2) Å.[3,32] The M–O bonds in **2-Sm** and **2-Eu** are shorter than in related anionic tris-(*tert*-butoxy)siloxide complexes of divalent Eu and Sm. In the complexes reported here, the bond distance to coordinated *tert*-butoxy oxygen ranges from 2.6381(19) to 2.6659(18) Å.[33] As expected, there is variation in the Si–O bond lengths within the structures of **2-Sm** and **2-Eu**, with the Si–O bond lengths for coordinated O atoms longer on average than the Si–O bond of non-coordinated O atoms. The average Si–O bond length for coordinated O atoms is 1.692(5) Å in both **2-Sm** and **2-Eu** compared to 1.634(5) Å for the non-coordinated O atoms.

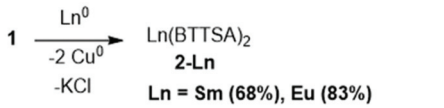

Scheme 2 Reaction scheme for the oxidation of zero-valent lanthanide metal with **1**.

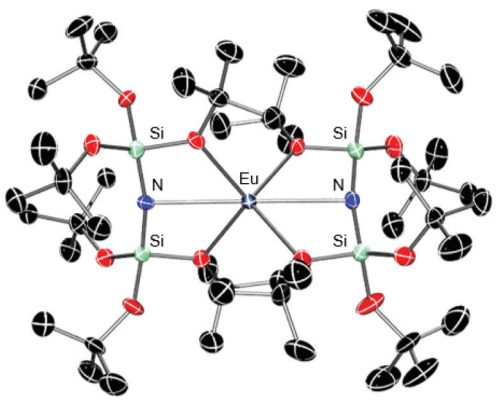

Fig. 1 Molecular structure of **2-Eu** with thermal ellipsoids shown at 50% probability with hydrogen atoms omitted for clarity.

Table 1 Selected bond lengths (Å) and angles (°) for **2-Sm** and **2-Eu**

	2-Sm	2-Eu
M–N (Å)	2.712(5)	2.7181(17)
M–O_{Coord} (Å)	2.540(5)	2.526(4)
Si–O_{Coord} (Å)	1.692(5)	1.692(5)
N–M–N (°)	179.21(14)	179.20(6)
Si–N–Si (°)	168.4(3)	169.6(1)

These divalent complexes present a near linear geometry along the N–M–N axis. The N–M–N bond angle is 179.21(14)° and 179.20(6)° for **2-Sm** and **2-Eu**, respectively. Additionally, the Si–N–Si bond angle in both complexes is more linear when compared to the structure for the proligand, **BTTSA-H**. When compared to analogous bis(tris-alkyl)silylamide complexes, this metric is significantly more linear. For example, bis(*tert*-butyl-dimethylsilyl)amine which has a Si–N–Si bond angle of 126.3(1)° in the lithium salt and 133.68° in the lanthanum complex,[31] while the Si–N–Si bond angle is 134.90(7)° in the pro-ligand, **BTTSA-H**, and 169.6(1)° and 168.4(3)° in the **2-Eu** and **2-Sm**, respectively. Similarly, in divalent Sm complexes supported by bis(tris-isopropyl)silylamides in $Sm[N(Si^iPr_3)_2]_2$, the Si–N–Si bond angles average 138.7(4).[3]

Since the N–M–N angles are nearly linear, the M–N bonds are notably long, and the M–O bond lengths are short, a τ_4 index for the "equatorial" O donors can quantify the extent of distortion.[34] For a perfect octahedron, this index would be 0.0 (*i.e.* square planar for the 4 oxygen donors). For both **2-Sm** and **2-Eu**, the index is calculated to be 0.89 – indicating strong distortion in the equatorial region of the coordination octahedron to a pseudo-tetrahedral geometry for the oxygen donors. This analysis is supported by the non-orthogonal relationship between the planes defined by the ONO donor atoms of each ligand which affords an angle between the planes of 89.3(3)° and 88.8(2)° for **2-Sm** and **2-Eu**, respectively.

The dc magnetic susceptibility data for **2-Sm** and **2-Eu** are shown in Fig. 2. The complex, **2-Sm**, has a $^7F_0$ ground state and a calculated room temperature moment of $0\mu_B$ based on Landé equations. However, a substantial moment is observed due to temperature-dependent population of low-lying excited j-states. This phenomenon also contributes to the general curve shape observed since as temperature increases, the gradual population of low-lying magnetic excited states increases. At room temperature, the moment for **2-Sm** is $3.45\mu_B$, and is consistent with the experimentally observed moments for other divalent samarium and isoelectronic Eu^{3+} compounds.[35] The complex, **2-Eu**, isoelectronic to Gd^{3+} complexes, has an isotropic $^8S_{7/2}$ ground state and exhibits a room temperature moment of $8.01\mu_B$, which is in good agreement with the expected moment for the ion of $7.94\mu_B$. In contrast to **2-Sm**, the moment remains constant from 300 K to 14 K, at which point the moment drops rapidly as it approaches 2 K. This behaviour can be rationalized since the f^7 ion contains

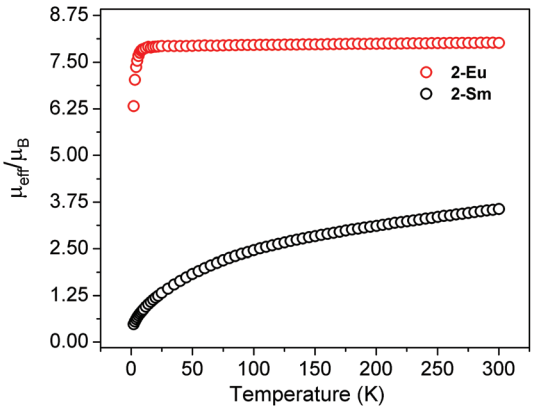

Fig. 2 Temperature dependence of magnetic moment (μ_{eff}) for **2-Sm** and **2-Eu** collected under dc field (H) of 1 T.

no low-lying excited j-states and the moment is purely produced through the population of the singular $^8S_{7/2}$ ground state.

Due to the stabilization of the 5d orbitals in the divalent lanthanides in comparison to their trivalent counterparts, spin-allowed f–d transitions give "traditional" divalent complexes (*i.e.* those with $4f^{n+1}$ ground state configurations) strong colors.[35] Divalent europium complexes are excluded, as these strong absorbances are typically centered in the UV and tail into the visible region giving them a pale color. The complexes **2-Sm** and **2-Eu** follow this trend: their solutions are deep forest green and pale lime green, respectively. Their UV-vis spectra in diethyl ether are shown in Fig. 3. The spectrum of **2-Sm** contains four noteworthy absorbance bands, ranging from a molar absorptivity of 350 to 1000 M^{-1} cm^{-1}, centred at 625 nm, 420 nm, 338 nm and 249 nm. The broad low energy peak at 625 nm is likely attributable to a $^7F_0$ to $^5D_0$ transition. The most intense feature for **2-Sm** is an imperfect Gaussian and appears to contain two contributing transitions, most likely $^7F_0$ to $^5D_1$ and $^7F_0$ to $^5D_2$ due to their proximity in energy. The higher energy transitions are more difficult to assign as they lie in a crowded manifold for metal-based transitions for a divalent samarium compound.[36] The spectrum for **2-Eu** contains two prominent absorbance bands, ranging from a molar absorptivity of 950 to 2500 M^{-1} cm^{-1} and centred at 335 and 284 nm, respectively. The feature at 335 nm is assignable as an $^8S_{7/2}$ to ^6P transition and the feature at 284 nm is an $^8S_{7/2}$ to ^6I transition. Despite the forbidden nature of these transitions, their molar absorptivity is substantially higher than what is observed for allowed transitions for **2-Sm**. This phenomenon has been noted previously for amide supported divalent europium complexes and has been suggested to be attributable to vibronic coupling in near linear coordination environments.[32] Such an analysis would suggest a strong topological homology between **2-Sm** and **2-Eu** and the $\{Ln[N(Si^iPr_3)_2]\}$ complexes.

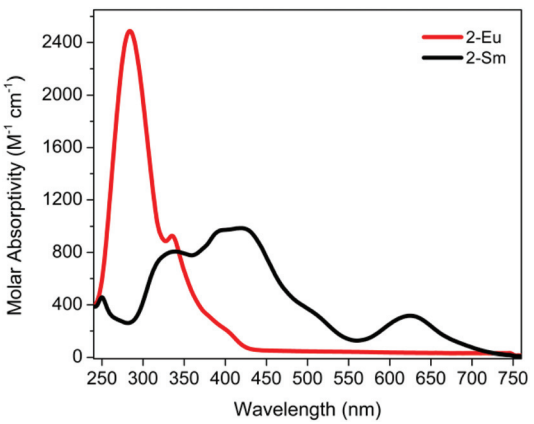

Fig. 3 UV-vis spectra of **2-Sm** and **2-Eu** in diethyl ether.

In summary, the synthesis and characterization of divalent complexes of Eu and Sm supported by the bulky, polydentate ligand bis(tris-*tert*-butoxysilyl)amide are reported. This synthetic approach is dependent on the use of a copper(I) species as an oxidative transmetallation reagent to prepare the neutral, divalent complexes directly from bulk metal as conventional metathesis reactions with lanthanide halides and alkali metal salts of BTTSA proved unsuccessful. Absorbance studies and variable-temperature dc magnetic susceptibility measurements confirm the divalent nature of the compounds and suggest that the observed distorted coordination polyhedra enforced by the linear Si–N–Si ligand backbone support a homologous structure to the formally two-coordinate $\{Ln[N(Si^iPr_3)_2]\}$ complexes.[3,32]

Conflicts of interest

There are no conflicts to declare.

Acknowledgements

Financial support was provided by the Georgia Institute of Technology and the Department of Energy, Heavy Element Chemistry Program (DE-SC0019385).

Notes and references

1 C. A. P. Goodwin, D. Reta, F. Ortu, N. F. Chilton and D. P. Mills, *J. Am. Chem. Soc.*, 2017, **139**, 18714–18724.
2 C. A. P. Goodwin, F. Ortu, D. Reta, N. F. Chilton and D. P. Mills, *Nature*, 2017, **548**, 439.
3 N. F. Chilton, C. A. P. Goodwin, D. P. Mills and R. E. P. Winpenny, *Chem. Commun.*, 2015, **51**, 101–103.
4 M. Xémard, M. Cordier, F. Molton, C. Duboc, B. Le Guennic, O. Maury, O. Cador and G. Nocton, *Inorg. Chem.*, 2019, **58**, 2872–2880.
5 M. Xémard, S. Zimmer, M. Cordier, V. Goudy, L. Ricard, C. Clavaguéra and G. Nocton, *J. Am. Chem. Soc.*, 2018, **140**, 14433–14439.

6 C. A. Gould, K. R. McClain, J. M. Yu, T. J. Groshens, F. Furche, B. G. Harvey and J. R. Long, *J. Am. Chem. Soc.*, 2019, **141**, 12967–12973.
7 J. D. Hilgar, M. G. Bernbeck, B. S. Flores and J. D. Rinehart, *Chem. Sci.*, 2018, **9**, 7204–7209.
8 M. S. Fataftah and D. E. Freedman, *Chem. Commun.*, 2018, **54**, 13773–13781.
9 M. Atzori and R. Sessoli, *J. Am. Chem. Soc.*, 2019, **141**, 11339–11352.
10 F.-S. Guo, B. M. Day, Y.-C. Chen, M.-L. Tong, A. Mansikkamäki and R. A. Layfield, *Angew. Chem., Int. Ed.*, 2017, **56**, 11445–11449.
11 J. D. Rinehart and J. R. Long, *Chem. Sci.*, 2011, **2**, 2078–2085.
12 A. N. Shoshkin, L. N. Bochkarev and S. Y. Khorshev, *Russ. J. Gen. Chem.*, 2002, **72**, 715–716.
13 L. N. Bochkarev, O. N. Druzhkova, S. F. Zhiltsov, L. N. Zakharov, G. K. Fukin, S. Y. Khorshev, A. I. Yanovsky and Y. T. Struchkov, *Organometallics*, 1997, **16**, 500–502.
14 W. J. Evans, *Polyhedron*, 1987, **6**, 803–835.
15 M. N. Bochkarev, L. N. Zakharov and G. S. Kalinina, *Organoderivatives of Rare Earth Elements*, Kluwer Academic, Dordrecht, 1995.
16 A. M. James, R. K. Laxman, F. R. Fronczek and A. W. Maverick, *Inorg. Chem.*, 1998, **37**, 3785–3791.
17 Y. F. Rad'kov, E. A. Fedorova, S. Ya. Khorshev, G. S. Kalinina, M. N. Bochkarev and G. A. Razuvaev, *Zh. Obshch. Khim.*, 1985, **55**, 2153.
18 A. E. Crease and P. Legzdins, *J. Chem. Soc., Chem. Commun.*, 1973, 775–776.
19 I. P. Beletskaya, G. Z. Suleimanov, R. R. Shifrina, R. Y. Mekhdiev, T. A. Agdamskii, V. N. Khandozhko and N. E. Kolobova, *J. Organomet. Chem.*, 1986, **299**, 239–244.
20 A. P. Ginsberg, *Inorganic Syntheses*, John Wiley & Sons, Inc, Hoboken, NJ, 1990, vol. 27, pp. 142–146.
21 H. D. Kaesz, *Inorganic Syntheses*, John Wiley & Sons, Inc, Hoboken, NJ, 1989, vol. 26, pp. 17–23.
22 F. T. Edelmann and W. A. Herrmann, *Synthetic Methods of Organometallic and Inorganic Chemistry*, Thieme Medical Publishers, Inc., New York, 1997, vol. 6, pp. 50–57.
23 H. Gilman and R. G. Jones, *J. Org. Chem.*, 1945, **10**, 505–515.
24 G. B. Deacon, M. G. Gardiner, P. C. Junk, J. P. Townley and J. Wang, *Organometallics*, 2012, **31**, 3857–3864.
25 G. B. Deacon, C. M. Forsyth and S. Nickel, *J. Organomet. Chem.*, 2002, **647**, 50–60.
26 C. R. Graves and J. L. Kiplinger, *Chem. Commun.*, 2009, 3831–3853.
27 A. J. Lewis, E. Nakamaru-Ogiso, J. M. Kikkawa, P. J. Carroll and E. J. Schelter, *Chem. Commun.*, 2012, **48**, 4977–4979.
28 C. R. Graves, B. L. Scott, D. E. Morris and J. L. Kiplinger, *J. Am. Chem. Soc.*, 2007, **129**, 11914–11915.
29 N. T. Rice, J. Su, T. P. Gompa, D. R. Russo, J. Telser, L. Palatinus, J. Bacsa, P. Yang, E. R. Batista and H. S. La Pierre, *Inorg. Chem.*, 2019, **58**, 5289–5304.
30 N. T. Rice, I. A. Popov, D. R. Russo, J. Bacsa, E. R. Batista, P. Yang, J. Telser and H. S. La Pierre, *J. Am. Chem. Soc.*, 2019, **141**, 13222–13233.
31 C. A. P. Goodwin, K. C. Joslin, S. J. Lockyer, A. Formanuik, G. A. Morris, F. Ortu, I. J. Vitorica-Yrezabal and D. P. Mills, *Organometallics*, 2015, **34**, 2314–2325.
32 C. A. P. Goodwin, N. F. Chilton, G. F. Vettese, E. Moreno Pineda, I. F. Crowe, J. W. Ziller, R. E. P. Winpenny, W. J. Evans and D. P. Mills, *Inorg. Chem.*, 2016, **55**, 10057–10067.
33 A. R. Willauer, D. Toniolo, F. Fadaei-Tirani, Y. Yang, M. Laurent and M. Mazzanti, *Dalton Trans.*, 2019, **48**, 6100–6110.
34 L. Yang, D. R. Powell and R. P. Houser, *Dalton Trans.*, 2007, 955–964.
35 K. R. Meihaus, M. E. Fieser, J. F. Corbey, W. J. Evans and J. R. Long, *J. Am. Chem. Soc.*, 2015, **137**, 9855–9860.
36 P. Hänninen and H. Härmä, *Lanthanide Luminescence: Photophysical, Analytical and Biological Aspects*, Springer, Berlin, 2013.